RESEARCH ARTICLE

Electrochemical Hydrogen Evolution Reaction Triggered by $Co_{2x}Mo_{1-x}S_2$ (x = 0. 0.05 and 0.1) in Acidic Medium

Aruna K Kunhiraman, Bradha Madhavan*

Facile solvothermal route was adopted for the synthesis of $Co_{2x}Mo_{1-x}S_2$ with x = 0, 0.05 and 0.1. Higher HER activity was exhibited by x = 0.1 in Co doped MoS_2, with a current density -140 $mAcm^{-2}$ at an overpotential of -100 mV. At lower overpotential both the compositions exhibited almost same activity, whereas with the increase in the overpotential and under continuous electrochemical operation, the active sites of composition with x = 0.1 was triggered and it was reflected in its HER activity.

Introduction

Incremental population and rising standards of living result in increase in the demand of energy. A decline in crude oil supply, political instability in the regions with large oil reserves and strict pollution regulation and control has created an alarming need for an alternative fuel. The alternate fuel should satisfy the criterion: (i) technical feasibility; (ii) environmental acceptability; (iii) reliable and safe availability; (iv) economically competitive; (v) inexhaustibility; and (vi) independent of primary energy sources. Among the various alternatives which include biodiesels, methanol, ethanol, hydrogen (H_2), boron, natural gas, liquefied petroleum gas (LPG), Fischer-Tropsch fuel, solar fuels etc.; H_2 takes the principal position. Thus, hydrogen energy system appears to be the one of the most effective solutions for sustainability and green environment with near-zero or zero liberation of greenhouse gases, if it is produced from renewable energy sources, such as wind, solar, nuclear and tidal [**1-2**]. H_2 is credited with advantages like: (i) high energy conversion efficiency; (ii) production from water with no emissions; (iii) abundance; (iv) different methods of storage (*e.g.* gaseous, liquid, or in together with metal hydrides); (v) long distance transportation; (vi) simplicity of conversion to other forms of energy and (vii) higher HHV (141.9 kJg^{-1}) and LHV (119.9 kJg^{-1}) than most of the conventional fossil fuels [**3**]. Thus, holding many economic and environmental benefits, H_2 will be the key contributor to the sustainable development as in future it will be produced in large quantities from renewable energy resources. Among the various routes for H_2 generation, electrochemical dissociation of water is regarded as the best way to generate pure form of hydrogen with zero liberation of global warming gases. The main blockade for the electrolyzer is the use of noble metals and their compounds catalyzing the hydrogen evolution reaction (HER) and the oxygen evolution reaction (OER) at the cathode side and the anode side of the electrolyzer respectively. Efficient cathode catalysts for hydrogen evolution reaction (HER) are the key to achieve optimal performance in water splitting.

Several non–noble metal materials, such as transition–metal chalcogenides [**4-7**], carbides [**8-10**], phosphides [**11,12**], nitrides [**13-15**] and oxides [**16-20**] are currently been tested as electrocatalyst for HER. 2D-chalcogenides have gained a wide range of attention among all the other new forms of electrocatalyst due to its amazing chemical and physical properties similar to graphene [**21,22**]. The co-ordination of Mo with S in 2H-MoS_2 is trigonal prismatic with Mo atoms sandwiched between S-atoms and are held together by strong Vander-Waals forces. Each Mo atom is surrounded by six S atoms in the form of a prism[23]. The basal planes of MoS_2 are always inactive whereas the edge sites are active toward HER activity [**24,25**]. Thus, creating more number of active sites at the edges will enhance the HER activity of the catalyst. Hinnemann *et al*. has reported that the activity sites in MoS_2 stems from the uncoordinated sulfur edges and its electrocatalytic activity for HER scales up linearly with the edge sites [**25,26**]. Since bulk MoS_2 is a poor electrocatalyst, henceforth researchers world-wide are putting efforts to enhance the electrochemical activity of MoS_2 by various means.

The synthesis strategies and routes of electrocatalyst are highly complicated at the outlay of expensive precursors. Even though a number of catalysts are developed to enhance the overall efficiency towards electrochemical water splitting but the routes of synthesis are complicated in which toxic and expensive precursors are used. Henceforth, we report a simple and environmental

Department of Science and Humanities, Rathinam Technical Campus, Eachanari, Coimbatore, Tamil Nadu 641021, India

*Corresponding author:
E-mail: arunakk2007@gmail.com; aruna.physics@rathinam.in

DOI: 10.5185/amlett.2021.081655

friendly solvothermal approach for the synthesis of Co doped MoS_2. The catalysts were characterized by X-ray diffraction (XRD), Raman spectroscopy and Transmission electron microscopy (TEM). A systematic comparison has been conducted with regard to $Co_{2x}Mo_{1-x}S_2$ (x = 0, 05 and 0.1) with Pt/C. All the electrochemical characterization of HER electrocatalysis like linear sweep voltammetry (LSV), Tafel polarization, and chronoamperometry (CA) has been performed and also turnover frequency (TOF) was calculated for the various compositions. The improvement in the HER activity for $Co_{2x}Mo_{1-x}S_2$, with x = 0.1 is due to the synergistic effect of Co ions in the MoS_2 hexagonal structure, creating large number of active and potent sites for the occurrence of HER.

Experimental

Materials

Sodium molybdate ($Na_2Mo_4.4H_2O$, ≥ 99.5%, Merck), potassium thiocyanate (KSCN, ≥ 98.5%, Merck), hydrazine hydrate ($N_2H_4.4H_2O$, 80%, ≥ Merck) and Cobalt Acetate ($(CH_3COO)_2Co.4\ H_2O$, 99.5%, Merck) were used for the synthesis. Nafion solution (5 wt.%, Fuel Cells Etc.) was used for catalyst ink preparation and pure graphite rods (M/S Nickunj Catalyzing Transformation India) was employed as counter electrode. Commercial platinum catalyst (20 wt. % Pt/C, Alfa-Aesar) was used for comparative HER activity studies. Ultrapure water (Resistivity: 18 Ωcm, Merck Millipore) was used throughout the experiment.

Synthesis and characterization of $Co_{2x}Mo_{1-x}S_2$ (x = 0, 0.05 and 0.1)

A facile one pot hydrothermal method was adopted for the synthesis of stand-alone MoS_2 as reported by Tian *et. al.*, [**27**]. Typically, 3.63 g $Na_2MoO_4.4H_2O$ and 3.66 g KSCN was mixed in 180 mL ultra-pure water. The mixture was then transferred to a 300 mL SS autoclave, sealed and maintained at a temperature of 260 ℃ for 24 h. The final product was obtained by filtration, washing and drying in a vacuum oven at 80 ℃ for 12 h. In order to synthesis Co doped MoS_2, calculated amount of $(CH_3COO)_2Co.4H_2O$ was added in the mixture of $Na_2MoO_4.4H_2O$ and KSCN before sealing in autoclave. 20 wt. % Pt/C was prepared by precursor reduction method. Chloroplatinic acid ($H_2PtCl_6.6H_2O$) was added slowly to Vulcan XC-72 carbon nanoparticles, which was pre-sonicated for 10-20 minutes in water and isopropanol mixture. pH of solution was maintained by adding 0.2 M Na_2CO_3. The end sample was filtered, washed with DD water and dried at 70 ℃ overnight.

Materials physicochemical and electrochemical characterization

The phase formations of the powders were confirmed by X-ray diffraction (XRD) using Shimadzu XRD-600 equipment. Microstructure and the morphological studies of the samples were obtained from transmission electron microscopy (TEM, JEOL JEM 2100). The electrocatalytic performance of the materials were analyzed from voltammetric plots, which were obtained using an M/S BioLogic Science electrochemical work station (VSP multichannel model) using a conventional three-electrode cell with glassy carbon electrode (GCE) as working electrode (W.E), mercury mercurous sulfate (MMS) as reference electrode and pure graphite rod as counter electrode respectively. The GCE was cleaned mechanically with various grades of alumina and diamond polishing liquid and finally washed thoroughly with DD water. Slurry to be coated onto the GCE was obtained by ultra-sonication of solution consisting 2.3 mg catalysts powder, 100 µl ethanol and 20 µl of 5 wt.% Nafion for half an hour. 5 µL homogeneously dispersed catalysts ink was pipetted out and drop casted onto the cleaned surface of the GCE having an active surface area of 0.071 cm2. The catalyst coated electrode was dried at 50 °C for 10 min. In order to gain insight into the electrocatalytic activity of catalyst materials, linear sweep voltammetry (LSV) within the potential region 0 mV to − 225 mV vs. RHE at $\nu = 10\ mVs^{-1}$ was performed. The stability of the catalysts was determined from chronoamperometry at an overpotential of -50 mV and accelerated degradation test (ADT) within a potential window 0 to -200 mV at $\nu = 100\ mVs^{-1}$ for 10,000 cycles. Tafel plots were obtained by running LSV in the low overpotential region at $\nu = 2\ mVs^{-1}$. Turn over frequency (TOF) was estimated by performing CVs, at non-faradaic regions at various scan rates. In order to have a global comparison, the obtained electrochemical results were calibrated with respect to the reversible hydrogen electrode (RHE) using the formula:

$$E_{RHE} = E_0 + 0.059 * (pH) + 0.625$$

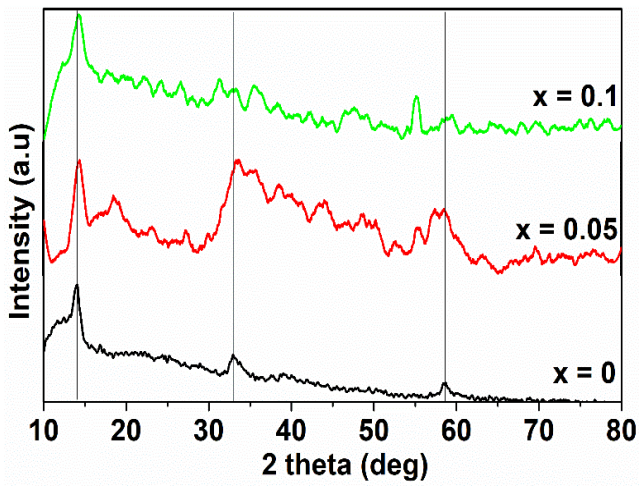

Fig 1. XRD pattern of $Co_{2x}Mo_{1-x}S_2$ with x = 0, 0.05 and 0.1

Results and discussion

The XRD patterns of MoS_2 and $Co_{2x}Mo_{1-x}S_2$ shown are shown in **Fig. 1**. The reduction in the crystallinity with the increase in the concentration of Co in MoS_2 structure is well clear by the presence of broad and low diffraction peaks.

All the major peaks of $Co_{2x}Mo_{1-x}S_2$ with x = 0, 0.05 and 0.1 were indexed using JCPDS file No: 37-1492, which reflects the characteristics peaks corresponding to 2H-MoS_2. Few secondary peaks were also observed with increase in the concentration of the Co doped in MoS_2. **Fig. 2** shows the TEM images of MoS_2 and Co doped MoS_2. Nanosheet formations were observed in MoS_2 as well in various composition of Co doped MoS_2. Curling and wrinkling of the structure exposes a greater number of active sites. The inset shows high resolution TEM images (HRTEM), which depicts the interlayers spacing of all the samples. **Fig. 3** shows the indexed SAED patterns, where brighter ring corresponding to (100) for MoS_2 and Co doped MoS_2 (x = 0.05) whereas the brighter ring for Co doped MoS_2, with x= 0.1. Thus, suggesting the preferential crystal growth along (100) for and (0004) for Co doped MoS_2, with x = 0.1. The ring formation in the SAED patterns uncovers the polycrystalline nature of MoS_2 and Co doped MoS_2 compositions.

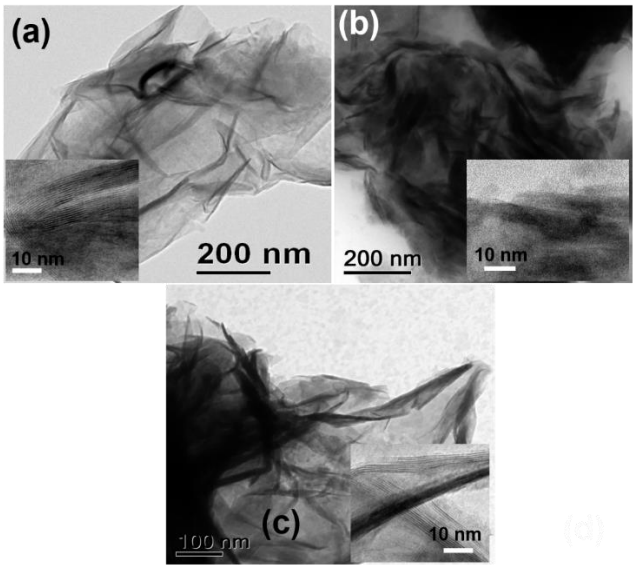

Fig 2. TEM images of Co doped MoS_2 with (a) x= 0, (b) x = 0.05 and (c) x = 0.1

The electrochemical studies were carried out for MoS_2 and two different compositions of $Co_{2x}Mo_{1-x}S_2$ with x = 0, 0.05 and 0.1. The activity of the electrocatalysts towards HER was evaluated from the polarization curves, which include the LSV, Tafel plots and chronoamperometry. **Fig. 4(a)** shows the polarization curves of 20 wt.% Pt/C and $Co_{2x}Mo_{1-x}S_2$ with x = 0, 0.05 and 0.1. The Figure reveals that $Co_{2x}Mo_{1-x}S_2$ with x = 0.1 is more active towards HER catalysis compared to x = 0 and 0.05. Even though the onset potential for both the catalysts remains the same (η = -30 mV), but with the increase in the overpotential, the catalytic activity of $Co_{2x}Mo_{1-x}S_2$ with x = 0.1 increases rapidly, thus claiming for more-number of active sites at higher overpotential. In order to attain a current density of -50 $mAcm^{-2}$, $Co_{2x}Mo_{1-x}S_2$ with x = 0.05 and 0.1, requires overpotential of -75mV and -68 mV respectively. 20 wt.% Pt/C, which is regarded as benchmark catalysts requires overpotential of -23 mV to attain a current density of -50 $mAcm^{-2}$.

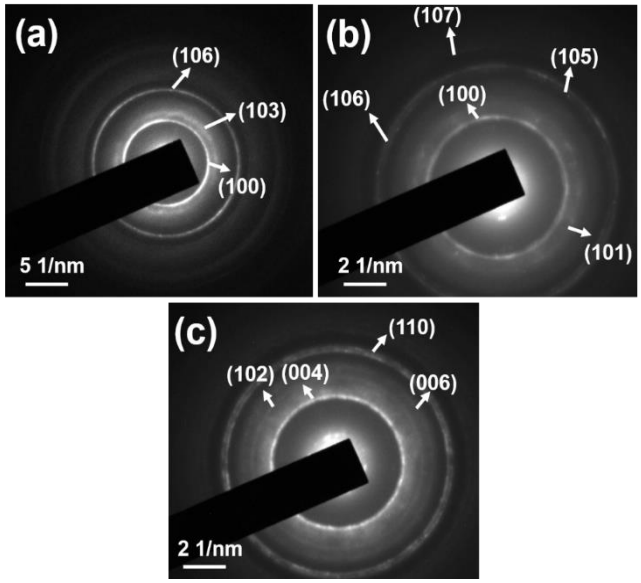

Fig 3. SAED pattern of Co doped MoS_2 with (a) x= 0, (b) x = 0.05 and (c) x = 0.1

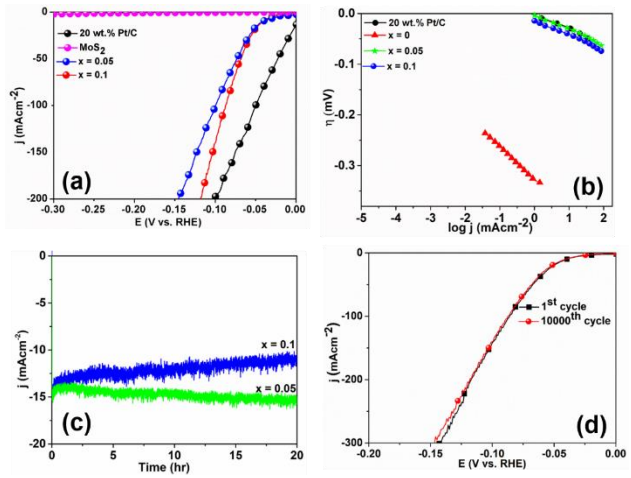

Fig. 4. (a) Polarization curves obtained at υ = 10 mVs^{-1} within the potential range 0 to -0.3 V, (b) 1st and 10000th cycle LSV for $Co_{2x}Mo_{1-x}S_2$ with x= 0.1 at υ = 2 mVs^{-1} (c) Tafel slope obtained at a υ = 2 mVs^{-1} and (d) chronoamperometric plots of $Co_{2x}Mo_{1-x}S_2$ with x= 0.05 and 0.1 at η = 50 mV.

Fig. 4(b) shows the further insight into the HER activity was obtained by Tafel plots depicted in **Fig. 4(c)**. The Tafel slope was determined by extrapolating the linear region. The slope of the linear region was used to find the b ($mVdec^{-1}$) values. The liberation of the H_2 from the surface of the W.E occurs *via* three possible mechanistic pathways taking place at the electrode/electrolyte interface. The mechanistic pathways are -

Discharge step:

$H_3O+ + e- \leftrightarrows S\text{-}H_{ads} + H_2O$
[Volmer step, b ≈ 120 mVdec^{-1}] (1)

Electrochemical desorption:

$S\text{-}H_{ads} + H_3O+ + e- \leftrightarrows H_2\uparrow + H_2O$
[Heyrovsky step, b ≈ 40 mVdec^{-1}] (2)

Chemical desorption:

$2S\text{-}H_{ads} \leftrightarrows H_2\uparrow$
[Tafel step, b ≈ 30 mVdec^{-1}] (3)

where, M denotes the surface empty site.

The electrochemical parameters derived from the LSV and Tafel are tabulated in the **Table 1**. The Tafel slope values remains the same for all the compositions and thus stands for the Volmer-Tafel as the rate determining step for the Catalysis of HER. In order to assess the stability of the catalyst, chronoamperometry was conducted continuously for 20 hr at η = -50 mV as shown in **Fig. 4(c)**. The composition with x = 0.1, showed enhancement in the activity with lapse in time, which indicates the activation of active sites during continuous operation. **Fig. 4(d)** shows the plot for 1st and 10000th cycle LSV, which also indicates the stability of the catalyst for the composition x = 0.1 in $Co_{2x}Mo_{1-x}S_2$.

Table 1. Electrochemical parameters derived from LSVs and Tafel plot:

Catalyst $Co_{2x}Mo_{1-x}S_2$	j (mAcm^{-2}) at η = -100 mV	η_{10} mV	Tafel (mVdec^{-1})
x = 0	-0.6	-	66
x = 0.05	-99	45	25
x = 0.10	-135	42	26
20 wt.% Pt/C	-197	1	30

Turn over frequency, TOF has been calculated in order to understand the intrinsic activity of the catalyst. TOF reflects the efficiency of the catalyst to generate H_2 pers second[5]. **Fig. 4** shows the CVs obtained in the non- faradaic region. The TOF at η = 10 mV for $Co_{2x}Mo_{1-x}S_2$ with x = 0.05 and 0.1 was calculated to be 0.12 s^{-1} and 0.7 s^{-1} respectively. Thus, the catalyst with composition x = 0.1 exhibits higher TOF and higher HER catalysis.

Conclusion

One pot solvothermal synthesis of $Co_{2x}Mo_{1-x}S_2$ with x = 0, 0.05 and 0.1 was studied and analyzed physiochemically and electrochemically toward HER activity. $Co_{2x}Mo_{1-x}S_2$ with x = 0.1 exhibited higher HER activity compared to other compositions. During continuous electrolysis under acidic environment large number of active sites were generated for x = 0.1 composition. In order to attain a current density of -50 mAcm^{-2}, $Co_{2x}Mo_{1-x}S_2$ with x = 0.05 and 0.1, requires overpotential of -75mV and -68 mV respectively. The stability of the catalysts was determined by running chronoamperometry at for 20 hrs at η = -50 mV. The rds of the system was derived to be Volmer-Tafel mechanism. Thus, further enhancement in the activity can be achieved by loading the composition with efficient support materials.

Acknowledgement

The support and the facilities extended by PSG Institute of Advanced Studies, Coimbatore, Tamilnadu, India is acknowledged.

Conflict of Interest

The author declares that there is no conflict of interest.

Keywords

MoS_2, chalcogens, hydrogen evolution reaction, electrocatalysis, doping

Received: 25 January 2021
Revised: 16 February 2021
Accepted: 27 March 2021

References

1. Momirlan, M.; Veziroglu, T. N., *Renew. Sustain. Energy Rev.*, **2002**, *6*, 141.
2. Turner, J. A.; Sustainable Hydrogen Production, *Science*, **2004**, *305*, 972.
3. Penner, S. S.; *Energy*, **2006**, *31*, 33.
4. Zheng, Z., et al., *Nat. Commun.*, **2020**, *11*, 3315.
5. Kunhiraman, A. K.; Ramanathan, S.; Pullithadathil, B.; *Electrochim. Acta*, **2018**, *264*, 329.
6. Wang, W.; Qiu, B.; Li, C.; Shen, X.; Tang, J.; Li, Y.; Liu, G.; *Electrocatalysis*, **2020**, *11*, 383.
7. Zhu, P.; Li, A.; Yang, Z.; Zhou, Y.; Xiong, X.; Ouyang, F.; *ACS Appl. Energy Mater.*, **2020**, *3*, 129.
8. Huang, J.; Hong, W.; Li, J.; Wang, B.; Liu, W.; *Sus. Energy & Fuels*, **2020**, *4*, 1078.
9. Chen, W.F.; Muckerman, J.T.; Fujita, E.; *Chem. Commun.*, **2013**, *49*, 8896.
10. Hussain, S.; Vikraman, D.; Feroze, A.; Song, W.; An, K.S.; Kim, H.S.; Chun, S.H.; Jung, J.; *Frontiers in Chem.*, **2019**, 7.
11. Chen, X.; Wang, D.; Wang, Z.; Zhou, P.; Wu, Z.; Jiang, F.; *Chem. Commun.*, **2014**, *50*, 11683.
12. Hu, C.; Lv, C.; Liu, S.; Shi, Y.; Song, J.; Zhang, Z.; Cai, J.; Watanabe, A.; *Catalysts*, **2020**, *10*, 188.
13. Song, F.; Li, W.; Yang, J.; Han, G.; Liao, P.; Sun, Y.; *Nat. Commun.*, **2018**, *9*, 4531.
14. Peng, X.; Pi, C.; Zhang, X.; Li, S.; Huo, K.; Chu, P. K.; *Sus. Energy & Fuels*, **2019**, *3*, 366.
15. Saad, A.; et al., *Nano-Micro Lett.*, **2020**, *12*, 79.
16. Kareem, A.; Kunhiraman, A. K.; Maiyalagan, T.; *Ionics*, **2020**, *26*, 5055.
17. Kalasapurayil Kunhiraman, A.; Ramasamy, M.; *J. Nanoparticle Res.*, **2017**, *19*, 203.
18. Zhu, Y.; Lin, Q.; Zhong, Y.; Tahini, H. A.; Shao, Z.; Wang, H.; *Energy & Environ. Science*, **2020**, *13*, 3361.
19. Wu, Y.; Sun, R.; Cen, J.; *Frontiers in Chem.*, **2020**, 8.
20. Li, Y., et al., *Frontiers in Mater.*, **2020**, 7.
21. Cao, J.; Zhou, J.; Zhang, Y.; Zou, Y.; Liu, X.; *PLOS One*, **2017**, *12*, e0177258.
22. Thangasamy, P.; Oh, S.; Nam, S.; Oh, I.K.; *Carbon*, **2020**, *158*, 216.
23. Eda, G.; Fujita, T.; Yamaguchi, H.; Voiry, D.; Chen, M.; Chhowalla, M.; *ACS Nano*, **2012**, *6*, 7311.
24. Jaramillo, T. F.; Jørgensen, K. P.; Bonde, J.; Nielsen, J. H.; Horch, S.; Chorkendorff, I.; *Science*, **2007**, *317*, 100.
25. Bonde, J.; Moses, P. G.; Jaramillo, T. F.; Nørskov, J. K.; Chorkendorff, I.; *Faraday Discuss.*, **2009**, *140*, 219.
26. Hinnemann, B.; Moses, P. G.; Bonde, J.; Jørgensen, K. P.; Nielsen, J. H.; Horch, S.; Chorkendorff, I.; Nørskov, J. K.; *Journal of the American Chemical Society*, **2005**, *127*, 5308.
27. Tian, Y.; He, Y.; Zhu, Y.; *Chem. Lett.*, **2003**, *32*, 768.